

# Novel Decentralized Pole Placement Design of Power System Stabilizers Using Hybrid Differential Evolution

YUNG-SUNG CHUANG	SHU-CHEN WANG	CHI-JUI WU	PEI-HWA HUANG
Department of Electrical Engineering Ming Hsin University of Science and Technology Hsin-Chu, TAIWAN jjs6869@must.edu.tw	Department of Computer and Communication Engineering Taipei College of Maritime Technology Taipei, TAIWAN scwang@mail.tcmt.edu.tw	Department of Electrical Engineering National Taiwan University of Science and Technology Taipei, TAIWAN cjwu@mail.ntust.edu.tw	Department of Electrical Engineering National Taiwan Ocean University Keelung, TAIWAN b0104@mail.ntou.edu.tw

*Abstract:* - This paper is used to investigate a novel decentralized pole placement design of lead-lag power system stabilizers using hybrid differential evolution (HDE). Since only local speed deviations are used as the feedback signals, the decentralized stabilizers could be easily implemented. It wants to place the electromechanical modes within a designated region to have enough damping. Participation factors are used to select the site and number of stabilizers. If all electromechanical modes have been moved to the specified region at the convergent step, the objective function will reach a minimal value. The objective function is chosen to ensure the real parts and damping ratios of electromechanical modes. A test power system is used to reveal the goodness of this method. Several operating points can be considered simultaneously in the determination of stabilizer parameters to let the stabilizers work well under a wider range of operating conditions. The computation time and convergence characteristic of this approach are better, compared to the differential evolution and genetic algorithm. The coherency measures are also proposed to evaluate the relative behaviours between any pair of generators of the system with and without stabilizers.

*Key-Words:* - Power system stabilizer, Electromechanical mode, Pole placement, Hybrid differential evolution, Power system dynamics, lead-lag power system stabilizers.

## 1 Introduction

The dynamic stability characteristics of a power system are affected by the location of electromechanical modes. It is sufficient that all electromechanical modes are placed in a suitable region in the complex variable plane to ensure damping effects on low frequency oscillations. Power system stabilizers (PSSs) have been widely used to increase the damping forces of electromechanical modes. Recently, design technology has been focused on how to tune PSSs in order to obtain suitable dynamic stability characteristics. Those methods include the optimization method using eigenvalue analysis [1], genetic design using simulated annealing optimization algorithms [2], probabilistic approach [3], Tabu search algorithm [4], particle-swarm-optimization technique [5], and genetic algorithm [6].

The hybrid differential evolution (HDE) is one of the best evolutionary algorithms for solving non-linear optimization problems [7]-[8]. A lot of works have been recoded about the applications of HDE. It

has been applied to the optimal control problem of a bio-process system [9]. Estimating the kinetic model parameters using HDE was presented in other literature [10]. It was also employed in plant scheduling and planning to solve the decision-making problems of the manufacturing industry [11]. The improved HDE method has been used to reduce power loss and enhance the voltage profile [12]. It may determine the optimal capacitor location of a radial distribution feeder [13].

The HDE is applied in this paper to tune the lead-lag type PSSs. Participation factors are used to determine the sites and number of PSSs [14]-[15]. The local generator speed feedback signals are applied to have decentralized control schemes [16]-[17]. It is to move all electromechanical modes to a designated region in the complex variable plane. The objective function is selected to ensure the real parts and damping ratios of electromechanical modes. At the convergent step, if all electromechanical modes have been moved to the designated region, the objective function will converge to zero, which is the minimal value. From the simulation results of a multi-machine power

system, the PSSs can let the generators have enough damping forces when there are line-tripping disturbances. The computation time and design results are better, compared with that using the differential evolution (DE) and genetic algorithm (GA). From the results of coherency measures, the levels of similarity between any pair of generators have been kept.

## 2 Hybrid Differential Evolution

A nonlinear optimization problem can be expressed as

$$\text{Minimize } M(\mathbf{X}) \quad (1)$$

Subject to

$$g_k(\mathbf{X}) \leq 0 \quad k = 1, \dots, n_g \quad (2)$$

$$h_k(\mathbf{X}) = 0 \quad k = 1, \dots, n_h \quad (3)$$

where  $M(\mathbf{X})$ : objective function of variable vector  $\mathbf{X}$ ,

$$\mathbf{X} = [\mathbf{X}_1, \mathbf{X}_2, \dots, \mathbf{X}_j, \dots, \mathbf{X}_D]^T$$

$g_k(\mathbf{X})$ : inequality constraints.

$h_k(\mathbf{X})$ : equality constraints.

Differential evolution is a parallel direct search method for minimizing nonlinear and non-differential objective functions. The fitness of an offspring is determined by one-to-one competition with the corresponding parent. The solution procedures are given as follows.

*Step 1. Initialization:* Several initial populations  $\mathbf{x}_i^0, i=1,2,\dots,N_p$  are randomly selected. They should cover the entire search space uniformly. The elements of each individual  $\mathbf{x}_i^0$  are given by

$$X_{ji}^0 = X_j^{\min} + \rho_i(X_j^{\max} - X_j^{\min}) \quad (4)$$

$$j = 1, 2, \dots, D, i = 1, 2, \dots, N_p$$

where  $\rho_i \in [0,1]$  is a random number, and  $N_p$  is the population size.  $X_j^{\min}$  and  $X_j^{\max}$  are the lower and upper bounds of the variable  $X_j$ , respectively.

*Step 2. Mutation operation:* At generation  $G$ , each mutant vector is generated based on the corresponding present individual  $\mathbf{x}_i^G$  by

$$\mathbf{U}_i^{G+1} = \mathbf{x}_i^G + F(\mathbf{x}_{r1}^G - \mathbf{x}_{r2}^G), \quad i=1,2,\dots,N_p \quad (5)$$

where  $i \neq r1, i \neq r2$ , and  $r1, r2 \in \{1, 2, \dots, N_p\}$ .

$F \in [0,1]$  is a scalar factor.  $\underline{x}_{r1}^G$  and  $\underline{x}_{r2}^G$  are two randomly selected individuals.

*Step 3. Crossover operation:* To extend the diversity of individuals in the next generation, the perturbed individual  $\mathbf{U}_i^{G+1} = [U_{1i}^{G+1}, U_{2i}^{G+1}, \dots, U_{ji}^{G+1}, \dots, U_{Di}^{G+1}]^T$  and the present individual  $\mathbf{x}_i^G = [X_{1i}^G, X_{2i}^G, \dots, X_{ji}^G, \dots, X_{Di}^G]^T$  are mixed to yield the trial vector

$$\hat{\mathbf{U}}_i^{G+1} = [\hat{U}_{1i}^{G+1}, \hat{U}_{2i}^{G+1}, \dots, \hat{U}_{ji}^{G+1}, \dots, \hat{U}_{Di}^{G+1}]^T \quad (6)$$

where

$$\hat{U}_{ji}^{G+1} = \begin{cases} X_{ji}^G, & \text{if a random number} > C_R \\ U_{ji}^{G+1}, & \text{otherwise} \end{cases} \quad (7)$$

$$j = 1, 2, \dots, D, i = 1, 2, \dots, N_p$$

where  $D$  is also the number of genes.  $C_R \in [0,1]$  is the crossover factor and must be set by the user.

*Step 4. Evaluation and selection:* The parent is replaced by its offspring in the next generation if the fitness of the latter is better. Contrarily, the parent is retained. The first step is one-to-one competition. The next step chooses the best individual,  $\mathbf{x}_b^{G+1}$  in the population. That is

$$\mathbf{x}_i^{G+1} = \arg\text{-min}\{M(\mathbf{x}_i^G), M(\hat{\mathbf{U}}_i^{G+1})\} \quad (8)$$

$$i = 1, 2, \dots, N_p$$

$$\mathbf{x}_b^{G+1} = \arg\text{-min}\{M(\mathbf{x}_i^{G+1}), i=1, 2, \dots, N_p\} \quad (9)$$

where  $\arg\text{-min}$  means the argument of the minimum.

The above steps are repeated until the maximum iteration number or the desired fitness is obtained. In general, a faster descent usually leads to a local minimum or a premature convergence. Conversely, diversity guarantees a high probability of obtaining the global optimum. The trade-off can be obtained by slightly lowering the scaling factor  $F$  and by

increasing the population size  $N_p$ . However, more computation time is required. The migrant and accelerated operations in HDE are used to overcome the local minimum solution and time consumption. The migrant and accelerating operations are inserted in the differential evolution.

*Step 5. Migrant operation if necessary:* For increasing search space exploration, a migration operation is introduced to regenerate a diverse population of individuals. The migrant individuals are selected on a “best individual” basis  $\mathbf{X}_b^{G+1}$ . The  $j^{\text{th}}$  gene of  $\mathbf{X}_i$  is regenerated by

$$X_{ji}^{G+1} = \begin{cases} X_{jb}^{G+1} + \rho_1(X_j^{\min} - X_{jb}^{G+1}), & \text{if a random number } \rho_2 < \frac{X_{jb}^{G+1} - X_j^{\min}}{X_j^{\max} - X_j^{\min}} \\ X_{jb}^{G+1} + \rho_1(X_j^{\max} - X_{jb}^{G+1}), & \text{otherwise} \end{cases} \quad (10)$$

where  $\rho_1$  and  $\rho_2$  are randomly generated numbers uniformly distributed in  $[0, 1]$ . The migrant population will not only become a set of newly promising solutions, but also avoid the local minimum trap.

The migrant operation is performed only if a measure fails to match the desired population diversity tolerance. The measure in this study is defined as

$$u = \frac{\sum_{i=1}^{N_p} \sum_{j=1}^D \eta_{ji}}{D(N_p - 1)} < \varepsilon_1 \quad (11)$$

where

$$\eta_{ji} = \begin{cases} 1, & \text{if } \left| \frac{X_{ji}^{G+1} - X_{jb}^{G+1}}{X_{jb}^{G+1}} \right| > \varepsilon_2 \\ 0, & \text{otherwise} \end{cases} \quad (12)$$

parameters  $\varepsilon_1 \in [0,1]$  and  $\varepsilon_2 \in [0,1]$  express the desired tolerance of the population diversity and the gene diversity with regard to the best individual, respectively. Here  $\eta_{ji}$  is defined as an index of the gene diversity. A zero  $\eta_{ji}$  means that the  $j^{\text{th}}$  gene of the  $i^{\text{th}}$  individual is close to the  $j^{\text{th}}$  gene of the best individual. If the degree of population diversity  $u$  is smaller than  $\varepsilon_1$ , the HDE performs migration to generate a new population to escape the local point.

Otherwise, HDE breaks off the migration, which maintains an ordinary search direction.

*Step 6. Accelerated operation if necessary:* When the fitness in the present generation is no longer improved using the mutation and crossover operations, a descent method is then applied to push the present best individual toward a better point. Thus, the acceleration operation can be expressed as

$$\hat{\mathbf{X}}_b^{G+1} = \begin{cases} \mathbf{X}_b^{G+1}, & \text{if a objective function } M(\mathbf{X}_b^{G+1}) < M(\mathbf{X}_b^G) \\ \mathbf{X}_b^{G+1} - \alpha \nabla M(\mathbf{X}_b^{G+1}), & \text{otherwise} \end{cases} \quad (13)$$

The gradient of the objective functions,  $\nabla M(\mathbf{X}_b^{G+1})$ , can be approximately calculated with a finite difference. The step size  $\alpha \in (0,1]$  is determined according to the decent property. Firstly,  $\alpha$  is set to unity. The objective function  $M(\hat{\mathbf{X}}_b^{G+1})$  is then compared with  $M(\mathbf{X}_b^{G+1})$ . If the decent property is achieved,  $\hat{\mathbf{X}}_b^{G+1}$  becomes a candidate in the next generation, and is added into this population to replace the worst individual. On the other hand, if the decent requirement fails, the step size is reduced, for example, 0.5 or 0.7. The decent search method is repeated to find the optimal  $\hat{\mathbf{X}}_b^{G+1}$ , called  $\mathbf{X}_b^N$ , at the  $(G+1)^{\text{th}}$  generation. This result shows the objective function  $M(\mathbf{X}_b^N)$  should be at least equal or smaller than  $M(\mathbf{X}_b^{G+1})$ .

### 3 Decentralized Pole Placement Design

#### Power system description

Determining the parameters of PSSs for an N-generator power system should consider various loading conditions. The equations of generator  $i$  in the linearized two-axis model are expressed by

$$\dot{\mathbf{x}}_i(t) = \mathbf{A}_{ii} \mathbf{x}_i(t) + \sum_{j=1, j \neq i}^N \mathbf{A}_{ij} \mathbf{x}_j(t) + \mathbf{B}_{ii} \mathbf{u}_i(t) \quad i=1,2,\dots,N \quad (14)$$

where  $\mathbf{x}_i(t) = [\Delta E'_{di} \quad \Delta E'_{qi} \quad \Delta \omega_i \quad \Delta \delta_i \quad \Delta E_{FDi} \quad \Delta V_{Si}]^T$  is the state vector,  $\Delta E'_{di}$  and  $\Delta E'_{qi}$  are the d-axis and q-axis transient voltages, respectively,  $\Delta \omega_i$  and  $\Delta \delta_i$  are the generator speed and angle, respectively,  $\Delta E_{FDi}$  is the field voltage, and  $\Delta V_{Si}$  is the output

signal of stabilizing transformer. The simplified static excitation system is given in Fig. 1.

**Lead-lag PSS**

The lead-lag phase compensation PSS is considered as shown in Fig. 2. The local generator speed deviations are used as the feedback signals. The transfer function is

$$u(s) = K_S \frac{sT_5}{1+sT_5} \left( \frac{(1+sT_1)(1+sT_3)}{(1+sT_2)(1+sT_4)} \right) \Delta\omega(s) \quad (15)$$

If the washout time constant,  $T_5$ , is given, the remaining parameters,  $K_S$ ,  $T_1$ ,  $T_2$ ,  $T_3$ , and  $T_4$ , are to be determined.

**Objective function**

The objective function is selected so that all electromechanical modes can be moved to the specified region as shown in Fig. 3. It is required that  $\sigma_{i,j} \leq \sigma_0$  and  $\zeta_{i,j} \geq \zeta_0$ , where  $\sigma_{i,j}$  and  $\zeta_{i,j}$  are the real part and damping ratio of the  $i$ th electromechanical mode under the  $j$ th operating condition. Then the objective function for an  $N$ -generator system is given by

$$M = \sum_{j=1}^{np} \sum_{i=1}^N (\sigma_0 - \sigma_{i,j})^2 + \sum_{j=1}^{np} \sum_{i=1}^N (\zeta_0 - \zeta_{i,j})^2 \quad (16)$$

for  $\sigma_{i,j} \geq \sigma_0$  and  $\zeta_{i,j} \leq \zeta_0$

where  $np$  is the number of operating points considered simultaneously in the design procedures. The system stability condition is determined by the damping constant,  $\sigma_0$ , and damping ratio,  $\zeta_0$ . In the design procedures using the HDE, the population size,  $N_P$ , is selected to be 5, the scalar factor,  $F$ , to be 0.01, and the crossover factor,  $C_R$ , to be 0.5.

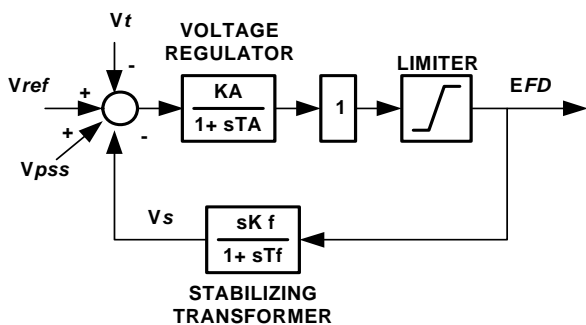


Fig. 1. Block diagram of static excitation system

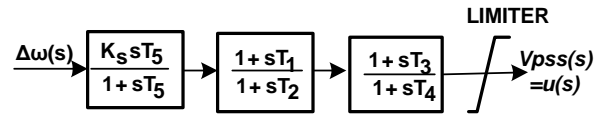


Fig. 2. Block diagram of lead-lag phase compensation power system stabilizer

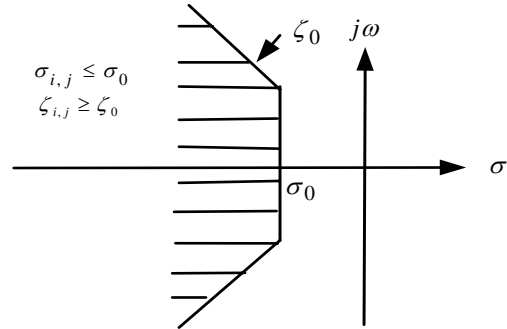


Fig. 3. A region where  $\sigma_{i,j} \leq \sigma_0$  and  $\zeta_{i,j} \geq \zeta_0$

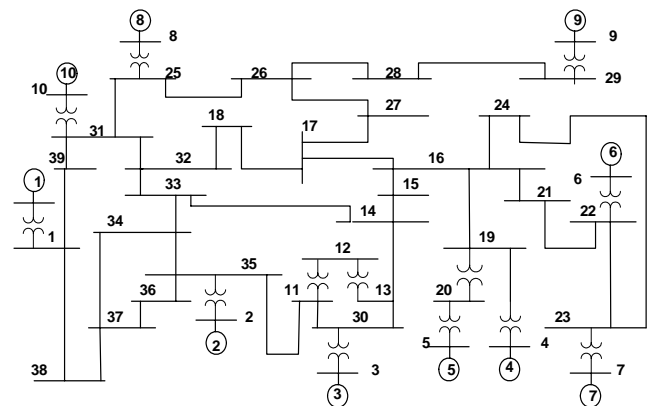


Fig. 4. The test power system

**4 Example: A Multi-machine System**

Consider the test power system as shown in Fig. 4 where bus 1 is assumed to be an infinite bus. Generators 2-10 (G2-G10) are equipped with static exciters. The system data are given in [18]. The electromechanical modes of the system are shown in the first column of Table 1. Some damping characteristics of electromechanical modes are poor, especially that of  $-0.06 \pm j6.68$  and  $-0.10 \pm j3.16$ .

The participation factors from summation of  $\Delta\delta$  and  $\Delta\omega$  of each generator associated with the electromechanical modes are also given in Table 1. G10 is chosen to install a PSS to enhance the worst damping mode  $-0.06 \pm j6.68$ . G9 is suitable to install a PSS and improve the mode  $-0.10 \pm j3.16$ . The other suitable sites are G2, G4 and G7.

### 4.1 Comparison of HDE, DE, and GA

In the designing PSSs of G2, G4, G7, G9, and G10 using DE, GA, and HDE, it is selected that  $\sigma_0 = -0.5$  and  $\zeta_0 = 0.1$ . The convergent results are revealed in Fig. 5. The computation time is evaluated by the CPU time as shown in Table 2. It indicates that HDE is faster than GA. Although DE is the fastest, it converges to a local optimal solution and has a larger convergent objective function. The designed parameters of PSSs are given in rows 2-4 of Table 3. The electromechanical modes of the system with DE\_PSS, GA\_PSS, and HDE\_PSS under operation condition 1 are tabulated in Table 4.

In the time domain simulations, nonlinear differential equations must be used to examine the damping effects of PSSs. The tripping of line 1-38 is used as a larger disturbance. Simulation results are given in Fig. 6 for generators 2, 4, 7, 9, and 10. The system with the HDE\_PSS has better responses.

### 4.2 Design under different operation conditions

In the design of PSSs using HDE, three operating conditions can be considered simultaneously.

Operating condition 1: Normal load.

Operating condition 2: Remove of line 1-38.

Operating condition 3: Remove of line 21-22, and 25 % load increase at buses 16 and 21, and 25% generation increase at G7.

It is also selected that  $\sigma_0 = -0.5$  and  $\zeta_0 = 0.1$ . Fig. 7 shows the comparison of convergent characteristic. The designed parameters of PSSs considering operation conditions 1-3 simultaneously are given in Table 5. The electromechanical modes designed under operating condition 1 only and operation condition 1-3 simultaneously are shown in the third row and fourth row of Table 6. For the system to have damping forces under a wider operation conditions, the designed PSSs under operation condition 1-3 simultaneously should be better than that under operation condition 1 only.

### 4.3 Comparison of different objective function

Two additional objective functions are compared with the M in (16).

(A) The objective function to emphasize the damping constants is

$$M_1 = \sum_{j=1}^{np} \sum_{i=1}^N (\sigma_0 - \sigma_{i,j})^2, \quad \text{for } \sigma_{i,j} \geq \sigma_0 \quad (17)$$

Table 1. Participation factors of generator speed and rotor angle of the system without PSS

Electromechanical mode (Damping Ratio)	G2	G3	G4	G5	G6	G7	G8	G9	G10
$-0.49 \pm j 9.48$ (0.05)	0	0	-0.16	-0.01	0.73	1.50	0	0	0
$-0.40 \pm j 9.21$ (0.04)	0	0	1.80	0.18	0.11	0.16	0.09	0	0
$-0.42 \pm j 8.80$ (0.05)	0.01	0.01	0.05	0.01	0.05	0	1.80	0.04	0.09
$-0.24 \pm j 7.99$ (0.03)	1.03	0.98	0	0	0	0	0	0	0
$-0.26 \pm j 7.08$ (0.04)	0.30	0.24	0.01	0.24	0.82	0.40	0	0.03	0.01
$-0.06 \pm j 6.68$ (0.01)	0.14	0.17	0	0.06	0.05	0.03	0.02	0.05	1.49
$-0.19 \pm j 6.03$ (0.03)	0.39	0.42	0	0.39	0.02	0.02	0.01	0.61	0.15
$-0.20 \pm j 5.91$ (0.04)	0	0	0.08	0.82	0.02	0.01	0.04	0.92	0.12
$-0.10 \pm j 3.20$ (0.03)	0.14	0.18	0.24	0.36	0.27	0.23	0.09	0.36	0.14

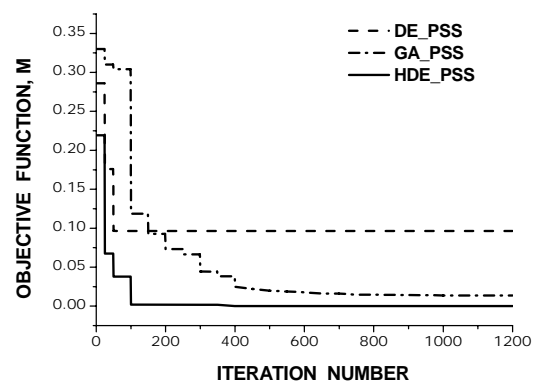


Fig. 5. Convergent characteristics of objective functions, M, using DE, GA, and HDE

A shape in which  $\sigma_{i,j} \leq \sigma_0$  is shown in Fig. 8. The design results want to force electromechanical modes to locate on the left side of the vertical line  $\sigma = \sigma_0$ .

(B) The objective function to emphasize the damping ratios is

$$M_2 = \sum_{j=1}^{np} \sum_{i=1}^N (\zeta_0 - \zeta_{i,j})^2, \text{ for } \zeta_{i,j} \leq \zeta_0 \quad (18)$$

This wants to put all electromechanical modes in a sector in which  $\zeta_{i,j} \geq \zeta_0$  as shown in Fig. 9 to ensure every electromagnetic mode has a damping ratio no less than the specified  $\zeta_0$ .

In the designing PSSs of G2, G4, G7, G9, and G10 using HDE considering operation conditions 1-3 simultaneously, it is also selected that  $\sigma_0 = -0.5$  and  $\zeta_0 = 0.1$ . Fig. 10 shows the comparison of convergent characteristics. The designed parameters of PSSs using  $M_1$  and  $M_2$  are given in Table 7. The electromechanical modes are given in the third, fourth, and fifth rows of Table 8, respectively. When the objective function  $M$  is used, the system has best dynamic characteristics.

#### 4.4 Coherency analysis

The coherency measures derived from responses in Fig. 6 are proposed to evaluate the relative behaviours between any pair of generators. The results are given in Table 9 and Table 10 for the system without and with the PSSs, respectively. It can be found that the levels of similarity have been kept. For example, the values in Table 9 show that G2 has a higher relation with G3. This situation also can be found in Table 10. Since the coherency behaviours do not be destroyed, the system should have a higher stability condition.

### 5 Conclusion

A comprehensive decentralized pole assignment method based on HDE has been successfully used in the design of lead-lag phase compensation power system stabilizers. A multi-machine system is used as an example to demonstrate the developed method and reveal the convergent procedures. The participation factors associated with the electromechanical modes are used to select the sites of power system stabilizers. The computation time and the convergent characteristics of the objective function are better, compared with that from GA and DE. The chosen region to assign the electromechanical modes could be relatively important in the design. From the simulation results, the HDE gives a good method in tuning power system stabilizers to improve system dynamic stability. The coherency analysis results reveal that the levels of similarity between any pair of generators have been kept.

Table 2. Comparison of DE, GA, and HDE

DE	Objective Function (pu)	$N_p$	CPU time (sec)	$C_R$	$F$
	0.0963	5	7.7776	0.5	0.01
GA	Objective Function (pu)	$N_p$	CPU time (sec)	$P_c$	$P_m$
	0.0138	5	293.4507	0.5	0.01
HDE	Objective Function (pu)	$N_p$	CPU time (sec)	$C_R$	$F$
	0.0002	5	76.8322	0.5	0.01

Table 3. Parameter values of PSSs designed under operation condition 1

		$K_S$	$T_1$ (sec)	$T_2$ (sec)	$T_3$ (sec)	$T_4$ (sec)	$T_5$ (sec)
DE	G2	21.1	0.97	0.13	0.85	1.02	0.50
	G4	7.14	1.80	0.22	0.79	0.02	0.50
	G7	39.5	1.80	0.01	0.86	0.78	0.50
	G9	16.1	1.78	1.78	0.66	1.88	0.50
	G10	18.6	1.81	0.17	1.66	0.44	0.50
GA	G2	45.3	1.66	0.69	1.08	0.26	0.50
	G4	18.4	0.02	0.57	0.03	1.88	0.50
	G7	48.7	1.08	0.01 9	1.43	1.45	0.50
	G9	49.6	1.53	0.55	1.35	0.14	0.50
	G10	49.5	1.80	0.24	1.99	0.25	0.50
HDE	G2	16.0	0.58	0.10	1.95	0.34	0.50
	G4	14.2	0.25	0.17	0.62	0.02	0.50
	G7	29.2	0.23	0.05	0.84	0.04	0.50
	G9	45.7	1.67	0.24	1.64	0.25	0.50
	G10	48.4	1.87	0.27	2.00	0.24	0.50

Table 4. Electromechanical modes with PSSs

DE	GA	HDE
Eigenvalue (Damping Ratio)	Eigenvalue (Damping Ratio)	Eigenvalue (Damping Ratio)
-3.19 ± j 7.41 (0.41)	-2.08 ± j 8.57 (0.24)	-2.30 ± j 7.64 (0.29)
-1.04 ± j 3.71 (0.27)	-1.28 ± j 4.90 (0.25)	-1.46 ± j 7.69 (0.19)
-0.82 ± j 2.38 (0.32)	-1.17 ± j 8.95 (0.13)	-1.28 ± j 8.55 (0.15)
-0.73 ± j 7.52 (0.10)	-1.11 ± j 6.42 (0.17)	-1.28 ± j 4.53 (0.27)
-0.43 ± j 7.02 (0.06)	-0.63 ± j 7.35 (0.09)	-1.04 ± j 9.34 (0.11)
-0.41 ± j 8.84 (0.05)	-0.59 ± j 8.92 (0.07)	-0.82 ± j 8.95 (0.09)
-0.38 ± j 8.19 (0.05)	-0.58 ± j 6.84 (0.08)	-0.82 ± j 8.95 (0.09)
-0.33 ± j 6.54 (0.05)	-0.57 ± j 9.22 (0.06)	-0.74 ± j 7.15 (0.10)
-0.33 ± j 5.95 (0.06)	-0.41 ± j 9.18 (0.04)	-0.68 ± j 6.43 (0.11)

Table 5. Parameter values of PSSs using HDE design under operation conditions 1-3

	$K_S$	$T_1$ (sec)	$T_2$ (sec)	$T_3$ (sec)	$T_4$ (sec)	$T_5$ (sec)
G2	26.4	1.37	0.01	1.19	1.07	0.50
G4	2.72	1.42	0.01	1.96	0.43	0.50
G7	22.8	0.96	0.35	1.03	0.01	0.50
G9	46.6	2.00	0.27	2.00	0.30	0.50
G10	43.9	1.99	0.29	2.00	0.20	0.50

Table 6. Electromechanical modes with PSSs using HDE design under operation condition 1 and operation condition 1-3

Design condition	under operation condition 1	under operation condition 1-3
Operation condition 1	-2.30 ± j 7.64 (0.29) -1.46 ± j 7.69 (0.19) -1.28 ± j 8.55 (0.15) -1.28 ± j 4.53 (0.27)	-2.20 ± j 4.16 (0.47) -2.02 ± j 5.54 (0.34) -2.01 ± j 8.01 (0.24) -1.41 ± j 9.16 (0.15)
Eigenvalue (Damping Ratio)	-1.04 ± j 9.34 (0.11) -0.82 ± j 8.95 (0.09) -0.82 ± j 8.95 (0.09) -0.74 ± j 7.15 (0.10) -0.68 ± j 6.43 (0.11)	-1.25 ± j 7.79 (0.16) -0.98 ± j 9.03 (0.11) -0.74 ± j 8.88 (0.08) -0.74 ± j 7.53 (0.10) -0.72 ± j 6.50 (0.11)
Operation condition 2	-2.32 ± j7.64 (0.30) -1.51 ± j4.43 (0.32) -1.43 ± j7.66 (0.18) -1.20 ± j8.45 (0.14)	-2.32 ± j 5.62 (0.38) -2.14 ± j 3.93 (0.48) -2.04 ± j 8.01 (0.25) -1.40 ± j 9.14 (0.15)
Eigenvalue (Damping Ratio)	-1.03 ± j9.32 (0.11) -0.98 ± j7.02 (0.14) -0.84 ± j8.84 (0.09) -0.78 ± j9.03 (0.09) -0.55 ± j6.29 (0.09)	-1.11 ± j 7.78 (0.14) -0.95 ± j 9.02 (0.10) -0.85 ± j 7.54 (0.11) -0.77 ± j 8.86 (0.09) -0.61 ± j 6.22 (0.10)
Operation condition 3	-2.29 ± j 7.57 (0.29) -1.82 ± j 7.93 (0.22) -1.23 ± j 8.54 (0.14) -1.20 ± j 4.02 (0.29)	-2.64 ± j 6.79 (0.36) -2.05 ± j 7.97 (0.25) -1.58 ± j 3.53 (0.41) -1.36 ± j 9.07 (0.15)
Eigenvalue (Damping Ratio)	-0.99 ± j 9.21 (0.11) -0.86 ± j 8.79 (0.10) -0.78 ± j 9.15 (0.08) -0.54 ± j 6.89 (0.08) -0.47 ± j 5.91 (0.08)	-1.12 ± j 7.82 (0.14) -0.87 ± j 8.79 (0.10) -0.84 ± j 9.10 (0.09) -0.76 ± j 6.82 (0.11) -0.63 ± j 5.97 (0.10)

Table 7. Parameter values of PSSs using HDE with different objective functions

Objective function		$K_S$	$T_1$ (sec)	$T_2$ (sec)	$T_3$ (sec)	$T_4$ (sec)	$T_5$ (sec)
$M_1$	G2	35.5	0.99	1.02	0.89	0.05	0.50
	G4	11.0	0.33	0.40	1.09	0.02	0.50
	G7	48.7	1.90	0.31	1.24	0.04	0.50
	G9	28.1	1.97	0.29	1.20	0.11	0.50
	G10	30.3	1.85	0.12	0.97	0.17	0.50
$M_2$	G2	25.5	1.41	1.64	1.96	0.03	0.50
	G4	5.08	0.65	0.10	0.54	0.01	0.50
	G7	14.1	0.78	0.12	1.22	0.02	0.50
	G9	50.0	2.00	0.27	1.65	0.25	0.50
	G10	37.6	2.00	0.20	1.76	0.22	0.50

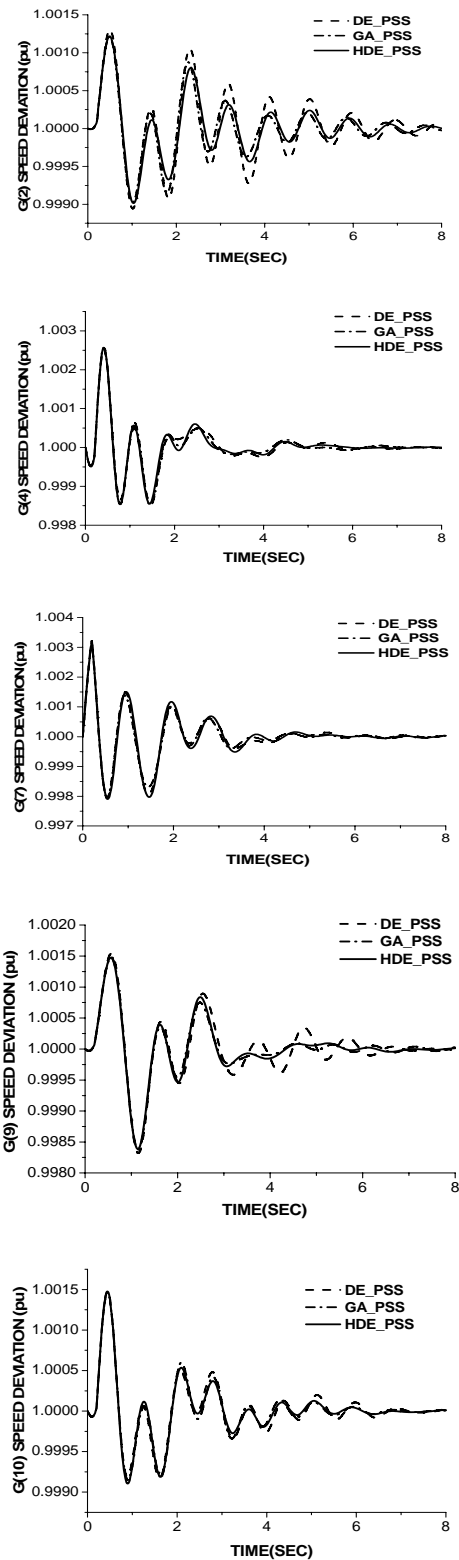


Fig. 6. Responses of Generators 2, 4, 7, 9, and 10 subjected to large disturbance

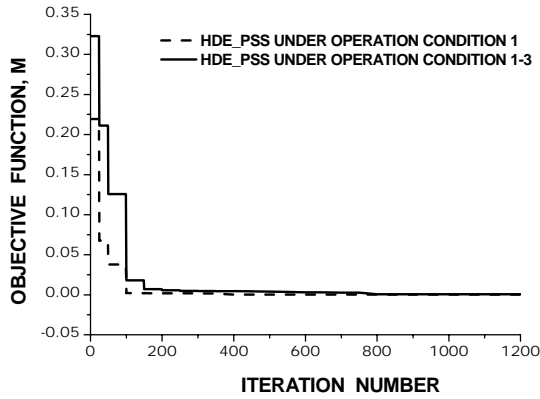


Fig. 7. Convergent characteristics of objective functions M using HDE under different operation conditions

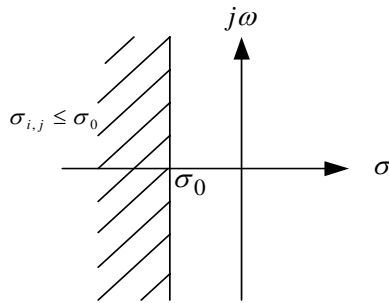


Fig. 8. A region where  $\sigma_{i,j} \leq \sigma_0$

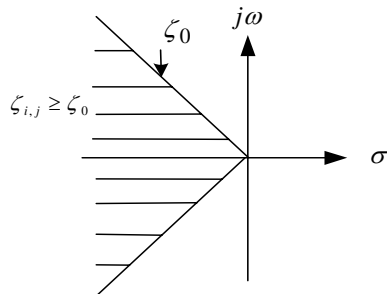


Fig. 9. A region where  $\zeta_{i,j} \geq \zeta_0$

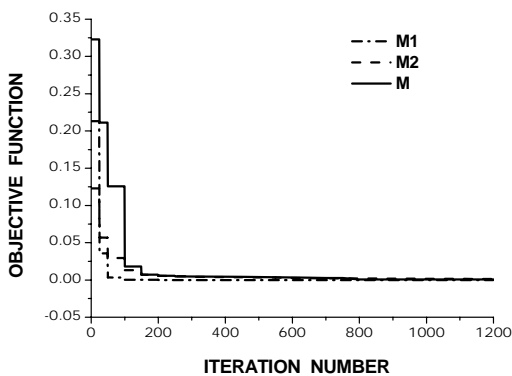


Fig. 10. Convergent characteristics of objective functions M, M1, and M2 using HDE

Table 8. Electromechanical modes using HDE with different objective functions designed under operation condition 1-3

Objective function	$M_1$	$M_2$	$M$
Operation condition 1	$-3.60 \pm j6.82$ (0.47)	$-2.29 \pm j8.15$ (0.27)	$-2.20 \pm j4.16$ (0.47)
	$-2.42 \pm j7.04$ (0.33)	$-1.46 \pm j8.95$ (0.16)	$-2.02 \pm j5.54$ (0.34)
	$-1.09 \pm j3.34$ (0.31)	$-1.40 \pm j7.96$ (0.17)	$-2.01 \pm j8.01$ (0.24)
	$-0.88 \pm j9.39$ (0.09)	$-1.23 \pm j4.10$ (0.29)	$-1.41 \pm j9.16$ (0.15)
	$-0.88 \pm j8.24$ (0.11)	$-0.98 \pm j8.95$ (0.11)	$-1.25 \pm j7.79$ (0.16)
	$-0.74 \pm j5.63$ (0.13)	$-0.84 \pm j5.91$ (0.14)	$-0.98 \pm j9.03$ (0.11)
	$-0.56 \pm j7.65$ (0.07)	$-0.76 \pm j7.66$ (0.10)	$-0.74 \pm j8.88$ (0.08)
	$-0.53 \pm j6.70$ (0.08)	$-0.79 \pm j6.76$ (0.12)	$-0.74 \pm j7.53$ (0.10)
	$-0.51 \pm j8.85$ (0.06)	$-0.65 \pm j8.86$ (0.07)	$-0.72 \pm j6.50$ (0.11)
	Operation condition 2	$-3.76 \pm j6.89$ (0.48)	$-2.32 \pm j8.15$ (0.27)
$-2.32 \pm j6.98$ (0.32)		$-1.44 \pm j8.92$ (0.16)	$-2.14 \pm j3.93$ (0.48)
$-0.98 \pm j3.09$ (0.30)		$-1.35 \pm j4.08$ (0.31)	$-2.04 \pm j8.01$ (0.25)
$-0.87 \pm j9.37$ (0.09)		$-1.25 \pm j7.94$ (0.16)	$-1.40 \pm j9.14$ (0.15)
$-0.85 \pm j5.70$ (0.15)		$-1.06 \pm j6.09$ (0.17)	$-1.11 \pm j7.78$ (0.14)
$-0.81 \pm j8.21$ (0.10)		$-0.98 \pm j8.94$ (0.11)	$-0.95 \pm j9.02$ (0.11)
$-0.57 \pm j7.63$ (0.07)		$-0.79 \pm j7.68$ (0.10)	$-0.85 \pm j7.54$ (0.11)
$-0.55 \pm j6.34$ (0.09)		$-0.65 \pm j8.85$ (0.07)	$-0.77 \pm j8.86$ (0.09)
$-0.51 \pm j8.84$ (0.06)		$-0.59 \pm j6.19$ (0.09)	$-0.61 \pm j6.22$ (0.10)

Table 9. Coherency measures of the system without PSS

	G2	G3	G4	G5	G6	G7	G8	G9	G10
G2	1.00	0.94	0.47	0.84	0.13	0.23	0.80	0.81	0.79
G3	0.94	1.00	0.50	0.82	0.14	0.23	0.84	0.78	0.82
G4	0.47	0.50	1.00	0.35	0.38	0.41	0.62	0.48	0.66
G5	0.84	0.82	0.35	1.00	0	0.11	0.67	0.77	0.65
G6	0.13	0.14	0.38	0	1.00	0.85	0.24	0.19	0.27
G7	0.23	0.23	0.41	0.11	0.85	1.00	0.32	0.31	0.35
G8	0.80	0.84	0.62	0.67	0.24	0.32	1.00	0.71	0.94
G9	0.81	0.78	0.48	0.77	0.19	0.31	0.71	1.00	0.72
G10	0.79	0.82	0.66	0.65	0.27	0.35	0.94	0.72	1.00



Table 10. Coherency measures of the system with PSSs

	G2	G3	G4	G5	G6	G7	G8	G0	G10
G2	1.00	0.87	0.62	0.78	0.20	0.33	0.82	0.84	0.83
G3	0.87	1.00	0.60	0.77	0.11	0.27	0.84	0.78	0.81
G4	0.62	0.60	1.00	0.45	0.30	0.45	0.70	0.59	0.75
G5	0.78	0.77	0.45	1.00	0	0.13	0.65	0.78	0.64
G6	0.20	0.11	0.30	0	1.00	0.82	0.22	0.18	0.27
G7	0.33	0.27	0.45	0.13	0.82	1.00	0.37	0.32	0.41
G8	0.82	0.84	0.70	0.65	0.22	0.37	1.00	0.70	0.92
G9	0.84	0.78	0.59	0.78	0.18	0.32	0.70	1.00	0.72
G10	0.83	0.81	0.75	0.64	0.27	0.41	0.92	0.72	1.00

#### Acknowledgments

The paper is partly supported by the Taipei College of Maritime Technology and the National Science Council of Taiwan, project number, NSC 95-2221-E-011-187.

#### References:

- [1] Y. Hong and W. Wu, A new approach using optimization for tuning parameters of power system stabilizers, *IEEE Transactions on Energy Conversion*, Vol. 14, No. 3, 1999, pp. 780-786.
- [2] M. Abido, Robust design of multimachine power system stabilizers using simulated annealing, *IEEE Transactions on Energy Conversion*, Vol. 15, No. 3, 2000, pp. 297-304.
- [3] C. Tse, K. Wang, C. Chung, and K. Tsang, Parameter optimization of robust power system stabilisers by probabilistic approach, *IEE Proceedings Generation, Transmission and Distribution*, Vol. 147, No. 2, 2000, pp. 69-75.
- [4] M. Abido and Y. Abdel-Magid, Robust design of multimachine power system stabilisers using Tabu search algorithm, *IEE Proceedings Generation, Transmission and Distribution*, Vol. 147, No. 6, 2000, pp. 387-394.
- [5] M. Abido, Optimal design of power system stabilizers using particle swarm optimization, *IEEE Transactions on Energy Conversion*, Vol. 17, No. 3, 2002, pp. 406-413.
- [6] Y. Abdel-Magid and M. Abido, Optimal multiobjective design of robust power system stabilizers using genetic algorithms, *IEEE Transaction on Power Systems*, Vol. 18, No. 3, 2003, pp. 1125-1132.
- [7] Y. Li, F. Wang, and K. Hwang, A hybrid method of evolutionary algorithms for mixed-integer nonlinear optimization problems, *Proceedings of the Congress on Evolutionary Computation*, Vol. 3, No. 1, 1999, pp.2159-2166.
- [8] Y. Lin, K. Hwang, and F. Wang, Hybrid differential evolution with multiplier updating method for nonlinear constrained optimization problems, *Proceedings of the Congress on Evolutionary Computation*, Vol. 1, No. 1, 2002, pp. 872-877.
- [9] J. Chiou and F. Wang, A hybrid method of differential evolution with application to optimal control problems of a bioprocess system, *Proceedings of the Congress on Evolutionary Computation*, Vol. 1, No. 1, 1998, pp. 627-632.
- [10] F. Wang and H. Jang, Parameter estimation of a bioreaction model by hybrid differential evolution, *Proceedings of the Congress on Evolutionary Computation*, Vol. 1, No. 1, 2000, pp. 410-417.
- [11] U. Lin, K. Hwang, and F. Wang, Plant scheduling and planning using mixed-integer hybrid differential evolution with multiplier updating, *Proceedings of the Congress on Evolutionary Computation*, Vol. 1, No. 1, 2000, pp. 593-600.
- [12] C. Su and C. Lee, Network reconfiguration of distribution systems using improved mixed-integer hybrid differential evolution, *IEEE Transactions on Power Delivery*, Vol. 18, No. 3, 2003, pp. 1022-1027.
- [13] C. Su and C. Lee, Modified differential evolution method for capacitor placement of distribution systems, *Asia Pacific IEEE/PES Transmission and Distribution Conference and Exhibition*, Vol. 1, No. 1, 2002, pp. 208-213.
- [14] T. L. Huang, K. T. Lee, C. H. Chang, and T. Y. Hwang, Sliding Mode Power System Stabilizer using Artificial Immune Algorithm, *WSEAS Transactions on Power Systems*, Vol. 1, No. 10, 2006, pp. 1707-1712.
- [15] J. R. Pacheco and J. Salinas, Modelling And Control Techniques For Tuning Stabilizers In Power Systems, *Proceedings of the 6th WSEAS International Conference on Circuits, Systems, Electronics, Control & Signal Processing (CSECS'07)*, Dec. 29-31, 2007, pp.239-244.
- [16] K. Turkoglu and E. M. Jafarov, Application of H inf. Loop Shaping Robust Control System Design on Longitudinal Dynamics of Hezarfen UAV with Classical PI(D) and Pole Placement Methods: A Comparison Analysis, *WSEAS Transactions on Power Systems*, Vol. 6, No. 1, 2007, pp. 206-213.
- [17] K. Zakova, Constrained Pole Assignment Controller for Delayed Double Integrator System, *Proceedings of the 6th WSEAS International Conference on System Science and Simulation in Engineering (ICOSSSE)*, Nov. 21-23, 2007, pp.12-17.
- [18] M. Pai, Energy function analysis for power system stability, Kluwer, Norwell, Massachusetts, 1989.